DISCUSSION OF THE BACK-BENDING EFFECT IN NUCLEI IN TERMS OF SIMPLE MODELS

By S. Ćwiok*, J. Dudek** and Z. Szymański

Institute of Nuclear Research, Warsaw***

(Received March 21, 1978)

The cranking method has been treated by means of the Hartree-Fock-Bogolyubov approach and has been applied to the description of fast nuclear rotation in terms of two simple models. The mechanism of the back-bending effect due to a gapless superconductivity, and closely connected with the Stephens-Simon alignment effect, was analysed. The yrast lines turn out to be composed mostly of the HFB vacuum states, however, some of the yrast states are shown to have two quasiparticle character. There is also another mechanism of the back-bending effect possible in our model; it is connected with the disappearance of the superfluid pairing correlations and occurs within the model provided the pairing is strong enough.

1. Introduction

The more detailed analysis of the multiband structure of rotational spectra has become possible owing to the recent progress in experiments on high angular momentum states in nuclei [1–3]. In some cases the identification of the crossing rotational bands connected with the back-bending effect has become possible in terms of the single particle orbitals [4–6] in line with the early suggestion by Stephens and Simon [7]. However, the presence of the short range correlations of the superfluid type [8] in nuclei tends to counteract the Coriolis and centrifugal forces [9]. Moreover, the possibility of the shape changes in the nucleus adds up to a rather complex picture of the nuclear processes at high angular momenta. In order to account for these effects properly the search was undertaken of the method general enough so as to incorporate all of the complex aspects of nuclear behaviour we mentioned above. It has been found that the Hartree-Fock-Bogolyubov (HFB) approach applied to the nuclear cranking model [10, 11] provides an appropriate scheme for the

* Address: Politechnika Warszawska, Koszykowa 75, 00-662 Warszawa, Poland.

** Address: Instytut Fizyki Teoretycznej, Uniwersytet Warszawski, Hoża 69, 00-681 Warszawa, Poland.

*** Address: Instytut Badań Jądrowych, Hoża 69, 00-681 Warszawa, Poland.

investigation of the high angular momentum processes in nuclei and, in particular, of the back-bending phenomena. This is sometimes referred to as "cranked HFB" method [12–16].

However, it has been argued that the cranking model procedure employing angular velocity of rotation, ω, leaves certain parts of the yrast line undefined [17, 18] (see also Refs [19, 20]). This is just the case if noninteracting single particle (or quasiparticle) picture is applied in the region where two levels cross as functions of ω. The elementary excitations may approximately be described in terms of single quasiparticles in the superfluid system. Crossing of the single quasiparticle eigenvalues, denoted from now on by E_L^{ω}, would then manifest itself as the effect of the gapless superconductivity [21, 22] and is closely related to the rearrangement of the quasiparticle vacuum state (see below). Following this line and thus including the two quasiparticle excited states in addition to the vacuum, Bengtsson and Frauendorf [4, 5] (see also [6]) have initiated an analysis of the high angular momentum rotational spectra. Recently, Bengtsson, Mottelson and Hamamoto [23] have found that the rearrangement of the HFB vacuum as connected with vanishing of the sum of two lowest quasiparticle eigenvalues occurs almost periodically as function of filling the $i\,\frac{13}{2}$ neutron shell in Rare Earth nuclei.

In this paper we attempt to analyse the band crossing within the cranked HFB method. In particular we concentrate on the structure of the HFB solutions near the point of rearrangement of the HFB vacuum and study in this way the structure of back-bending effect. We use the simple model in which a rather detailed analysis of the solution properties becomes possible. Following the discussion of Hamamoto [18], regions of the yrast line that are undefined by the single quasiparticle cranking model are filled in by the two quasiparticle states obtained from HFB equations, similarly as in the calculation by Bengtsson and Frauendorf [4, 5]. One may hope that after having understood the role of the gapless superconductivity (or the effect of crossing) in the microstructure of the yrast line one may be able to describe adequately the nuclear behaviour in the whole region of back-bending.

We shall start our considerations by recapitulating the main assumptions underlying the cranking model procedure (Section 2). Then, (Section 3), we employ a very simple model based on the two level solution of the HFB equations [24] (see also [25]) and we discuss the level crossing. Next, (Section 4) we present another model employing the $i\,\frac{13}{2}$ multiplet located in the vicinity of levels that are less sensitive to nuclear rotation than those of $i\,\frac{13}{2}$.

2. *Cranking model*

In this section we shall briefly recall the procedure of minimization of the nuclear energy for fixed angular momentum. This leads to one of the possible formulations of the cranking model. We assume that the nucleus is described by the Hamiltonian H including the deformed single particle potential V and the two-body monopole pairing forces of strength G. Although the HFB method provides us, in principle, with the possibility of deriving the selfconsistent potential from the realistic two-body forces, we shall not be

concerned with this part of the problem assuming that our potential V is already selfconsistent. We focus our attention on the properties of the gap (order) parameter Δ characterising the selfconsistent behaviour of the pairing force (see below).

We minimize the energy defined as the expectation value of the hamiltonian H with the constraint that the total angular momentum (which is identified throughout this paper with the component J_x, an approximation valid for large angular momenta we are especially interested in) has a definite value $\hbar\sqrt{I(I+1)}$. In this way we are led to the auxiliary (cranking) operator H^ω in the form

$$H^\omega = H - \omega' \hbar J_x, \tag{2.1}$$

where the Lagrange multiplier ω' has in addition the physical meaning of the angular velocity of rotation so that we can write

$$\omega' = \omega = (1/\hbar)\, dE/d(\sqrt{I(I+1)}).$$

Here, E is the total nuclear energy i. e. including also the energy of rotation (see bellow). Operator H^ω of Eq. (2.1) may be understood alternatively as the Hamiltonian of the system rotating with angular velocity ω about the x-axis. The presence of the $\omega\hbar J_x$ term in H^ω accounts for the Coriolis and centrifugal forces in nuclei. Hamiltonian of the system, H, is taken to be a sum of the single particle kinetic energy and the deformed potential energy terms and the two-body monopole pairing force expressed by

$$V_p = -G \sum_{k,k'} a_k^\dagger a_{\bar{k}}^\dagger a_{\bar{k}'} a_{k'} \tag{2.3}$$

in the standard notation ($|\bar{k}\rangle$ is time reversed $|k\rangle$).

Now, diagonalisation of H^ω leads to determination of the eigenvalues E^ω

$$H^\omega |\psi^\omega\rangle = E^\omega |\psi^\omega\rangle \tag{2.4}$$

while the parameter ω has to be calculated from the constraint equation

$$\langle \psi^\omega | J_x | \psi^\omega \rangle = \sqrt{I(I+1)} \tag{2.5}$$

whose solutions provide us with the dependence $\omega = \omega(I)$.

It is very difficult to find exact solutions of Eqs (2.4) even for simplified models. If the HFB approximation is used, equation (2.5) has to be completed by two additional relations. One of them is the particle number equation

$$N = \sum_k \varrho_{kk} \tag{2.6}$$

and the second is the gap equation

$$\Delta = 2G \sum_k \chi_{k\bar{k}}. \tag{2.7}$$

Here ϱ and χ denote density and pair density matrices defined as usually in the HFB formalism (see e. g. Ref. [26]). Two equations, Eq. (2.6) and Eq. (2.7), are used for determining the chemical potential λ and the gap parameter Δ.

The operator H^ω is only the auxiliary Hamiltonian which should not be identified with the energy if $\omega \neq 0$. The true nuclear energy, E, is calculated as the expectation value of the original Hamiltonian H in the state $|\psi^\omega\rangle$

$$E = \langle\psi^\omega|H|\psi^\omega\rangle = E^\omega + \hbar\omega\sqrt{I(I+1)}\,. \tag{2.8}$$

Let us also observe that

$$dE^\omega/d\omega = -\hbar\sqrt{I(I+1)}. \tag{2.9}$$

It often happens, in the typical nuclear HFB calculation, that structure of the HFB vacuum state $|\psi^\omega\rangle$ is abruptly changed at certain value of ω. Then the curve E^ω versus ω undergoes a rapid change in slope or even a cusp. This corresponds, in the case of an unpaired system, to a crossing of the two single particle eigenvalues of H^ω at this ω value [27]. Although there may be no discontinuity in E^ω with respect to ω, a jump in the value of $\sqrt{I(I+1)}$ must follow from the abrupt change of the vacuum structure. Energy E becomes then a discontinuous function of ω (cf. Eq. (2.8)) and the plot of E versus I (yrast line) exhibits a gap corresponding to the discontinuity in both E and I near the point of the band crossing.

3. Model based on a pair of the two-level systems

We shall first consider the simple solvable model consisting of the two subsystems, denoted in the following by I and II, both of the two-level type. Subsystem I consists of four levels, say *1*, *2*, *3* and *4*, where *2* is time reversed *1* and *4* is time reversed *3*. The split-

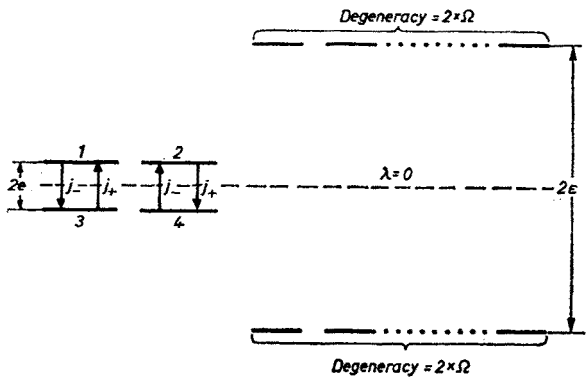

Fig. 1. Simple model for a single $j = 3/2$ shell (states 1, 2, 3, 4 split by "deformation") embedded in the opposite parity spectrum (2Ω degenerate two level model) as discussed in the text

ting between the levels *1*, *2* and *3*, *4* is denoted by $2e$, Fig. 1. We assume that the j_x operator (single particle component of J_x) connects the states *1* with *3* and *2* with *4* only, so that

$$(j_x)_{13} = (j_x)_{31} = -(j_x)_{24} = -(j_x)_{42} = 1 \tag{3.1}$$

while all the other matrix elements vanish by definition. Subsystem II is composed of

4Ω states forming two degenerate levels split by energy 2ε. Each pair of levels is now 2Ω times degenerate. These states, by the assumption, do not interact either among themselves or with the levels of subsystem I via j_x operator. The purpose of introducing the subsystem II is to provide the appropriate density of levels so as to create the superfluid correlations in the system while the presence of Coriolis interaction between states *1*, *2*, *3* and *4* of subsystem I serves for exhibiting those properties of the whole system that are most sensitive to nuclear rotation. We assume furthermore that the number of particles in the system is $N = 2\Omega+2$, i. e. corresponds to the one half of the available levels, $N_1 = 4\Omega+4$. We also assume that both subsystems, I and II, are located symmetrically with respect to zero energy so that $e_k = +e$ for levels *1* and *2* and $e_k = -e$ for levels *3* and *4*, while $e_k = +\varepsilon$ or $-\varepsilon$ for the upper and lower parts of subsystem II, respectively. This symmetry implies that the location of the chemical potential is fixed at $\lambda = 0$ when we apply the HFB method. Note that $\lambda = 0$ holds independently of ω in the model.

Let us now develop cranking model for the system using the HFB method. Solutions of the HFB equations for subsystem I treated separately are known [24] (see also [25]). In our case the two subsystems are not coupled by Coriolis interaction. The only coupling between the two subsystems is provided by the requirement of selfconsistency i. e. by the gap equation (2.7). As mentioned before the two body pairing force is assumed to be of the pure monopole nature which implies that the pairing force affects HFB equations only through the one parameter, Δ. We shall not write down the HFB equations in this section but rather in Section 4 where a slightly more complicated model is discussed (see also Refs [4, 5, 12–16]). For the two level model (subsystem I) the HFB equations have been solved explicitly (see Refs [24, 25] and also Refs [19, 28]). Our notation follows here generally the one of Ref. [28]. The quasiparticle eigenvalues corresponding to the subsystem I are

$$E_{\pm} = \sqrt{e^2+(\Delta \pm \hbar\omega)^2}. \tag{3.2}$$

It can easily be shown that for the subsystem II we obtain the familiar BCS-type wave function. Consequently the quasiparticle energies are

$$\mathscr{E} = \sqrt{\varepsilon^2+\Delta^2}. \tag{3.3}$$

The HFB density matrix $\varrho_{kk'}$ and the pair density matrix $\chi_{kk'}$ turn out to be block diagonal with respect to subsystems I and II and both parts of ϱ and χ can be written down explicitly. The corresponding matrices for the subsystem I are given e. g. in Table (2–2) of Ref. [28]. For the system II simple BCS formulas are valid

$$\varrho_{kk'} = \delta_{kk'} \sqrt{(1-e_k/\mathscr{E})/2}\,, \tag{3.4}$$

$$\chi_{kk'} = \delta_{k\bar{k}'} \operatorname{sgn}(k) \tfrac{1}{2} \sqrt{(1-e_k/\mathscr{E})(1+e_k/\mathscr{E})}\,, \tag{3.5}$$

where $e_k = \pm\varepsilon$ for the upper and lower level, respectively and $\mathscr{E}$ is given by Eq. (3.3).

Now the selfconsistency conditions read

$$2\Delta/G = (\Delta+\hbar\omega)/E_+ + (\Delta-\hbar\omega)/E_- \tag{3.6}$$

(gap equation) and

$$\hat{I} = (\Delta+\hbar\omega)/E_+ - (\Delta-\hbar\omega)/E_- \tag{3.7}$$

(angular momentum equation), where

$$\hat{I} = \sqrt{I(I+1)}. \tag{3.8}$$

The function E^ω corresponds to the vacuum state energy and is given in the HFB formalism (see for instance Ref. [26]) as

$$\begin{aligned} E^\omega &= \langle \psi^\omega | H^\omega | \psi^\omega \rangle \\ &= \sum_{kk'} [e_k \delta_{kk'} - \omega (j_x)_{kk'}] \varrho_{kk'} - \tfrac{1}{2} \Delta \sum_k \chi_{k\bar{k}} \end{aligned} \tag{3.9}$$

in terms of the ϱ and χ matrices. In the discussed model one can calculate E^ω explicitly. The result is

$$E^\omega = \Delta^2/G - 2\Omega\mathscr{E} - E_+ - E_-. \tag{3.10}$$

Let us now discuss properties of the solutions to the model described above and consider first an approximate solution in the case of large degeneracy of levels in the subsystem II: $\Omega \gg 1$. The subsystem I can then be treated as a small perturbation. We may use expansions

$$\Delta = \Delta_0 + \Delta_1 + \ldots, \tag{3.11}$$

$$\mathscr{E} = \mathscr{E}_0 + \mathscr{E}_1 + \ldots, \tag{3.12}$$

where

$$\mathscr{E}_0 = G\Omega, \tag{3.13}$$

$$\Delta_0 = \sqrt{(G\Omega)^2 - \varepsilon^2}, \tag{3.14}$$

are the zero order solutions of Eq. (3.6). The first order expression is

$$\begin{aligned} \mathscr{E}_1 &= [G^2\Omega/(2\Delta_0)]\,[(\Delta_0+\hbar\omega)/E_+^{(0)} + (\Delta_0-\hbar\omega)/E_-^{(0)}] \\ &= \Delta_0\Delta_1/\mathscr{E}_0, \end{aligned} \tag{3.15}$$

where

$$E_\pm^{(0)} = (E_\pm)|_{\Delta=\Delta_0}. \tag{3.16}$$

Using Eq. (3.9) we obtain, to first order,

$$E^\omega = -(G\Omega^2)\,\{1+[\varepsilon/(G\Omega)^2]\} - (E_+^{(0)} + E_-^{(0)}) + \ldots. \tag{3.17}$$

Equalities (3.11)–(3.17) exhibit smooth behaviour of HFB vacuum as a function of ω. The variation, however, of all relevant functions becomes quite rapid when the energy splitting, e, in subsystem I is small i. e.

$$e \ll \Delta_0. \tag{3.18}$$

In this case we have esentially $\hat{I} \approx 0$ for $\omega < \Delta_0/\hbar$ while for $\omega > \Delta_0/\hbar$ we obtain $\hat{I} \approx 2$ (cf. Eq. (3.7)). This behaviour leads to a rapid increase of the total energy (2.8) as function of ω, in addition to the jump in $\hat{I}$. The quasiparticle spectrum and the energy E as a function of ω are illustrated in Fig. 2 with solid lines.

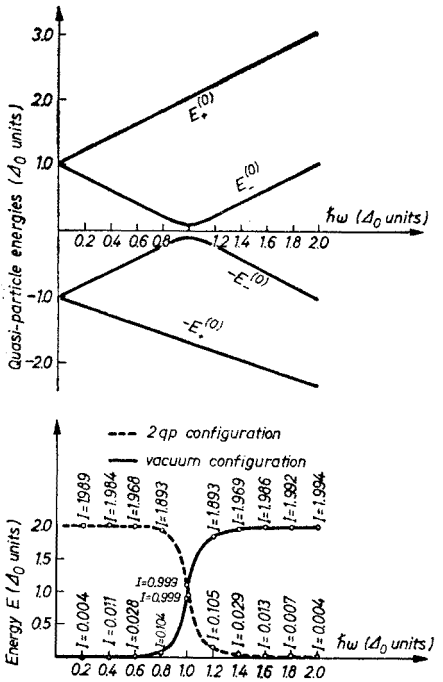

Fig. 2. Quasiparticle energies of the single "$j = 3/2$ shell" model (upper part) and the corresponding total energies of the vacuum (solid line) as well as 2 q. p. configuration (dashed line) vs angular velocity. Numbers along the total energy curves denote angular momentum

Let us consider, in addition to the ground state (i. e. the HFB vacuum state) also the excited two quasiparticle state obtained by making use of the negative energy solution for the quasiparticle energy [12]

$$E = -E_- \tag{3.19}$$

which should replace now the positive one included previously ($E = +E_-$). Thus we obtain other solutions of the HFB equations and in particular the eigenvectors obtained now differ from those obtained previously. As a consequence we obtain modified matrices ϱ and χ as well. These matrices can be expiessed from Table (2–2) of Ref. [28] by interchanging E_- and $(-E_-)$. In this way we obtain modified expressions also for Δ, E^{ω} and E which correspond to the two quasiparticle excited state. In the approximation $\Omega \gg 1$ we get

$$E^{\omega}_{2\text{q.p.}} = -(G\Omega^2)\{1+[\varepsilon/(G\Omega)^2]\} - (E^{(0)}_+ - E^{(0)}_-) + \ldots . \tag{3.20}$$

The total energy E (cf. Eq. (2.8)) which results from considering of the two quasiparticle state is illustrated in Fig. 2 (dashed line). Let us observe that in our approximation both curves, E and $E^{\omega}_{2q.p}$, for vacuum and two quasiparticle state respectively, are symmetric with respect to $\omega = \Delta_0/\hbar$. This symmetry follows directly from the fact that our subsystem II is completely insensitive to nuclear rotation and the only change with ω is provided by the ω-dependent mixture of the upper branch ($\hat{I} = 2$) with the lower one ($\hat{I} = 0$), Fig. 2. In fact, the more realistic (ω-dependent) subsystem II would produce an asymmetry in Fig. 2 (bottom part) by tilting the whole picture counterclockwise about a certain angle.

We can also calculate the dispersion in angular momentum j_x corresponding to our simple model. For $\Omega \gg 1$ we obtain

$$D(\omega) \overset{\text{df}}{=} \langle \psi^{\omega} | J_x^2 | \psi^{\omega} \rangle - \langle \psi^{\omega} | J_x | \psi^{\omega} \rangle^2$$

$$= e^2 \left(\frac{1}{E_+^2} + \frac{1}{E_-^2} \right) = e^2 \left(\frac{1}{E_+^{(0)2}} + \frac{1}{E_-^{(0)2}} \right) + \ldots \tag{3.21}$$

If $e \ll \Delta_0$, dispersion (3.21) is generally a very small quantity except for the immediate vicinity of the point $\omega = \Delta_0/\hbar$ where

$$D(\omega = \Delta_0/\hbar) \approx \frac{2e^2 + 4\Delta_0^2}{e^2 + 4\Delta_0^2} \approx 1. \tag{3.22}$$

Variation of the dispersion D is illustrated in Fig. 3.

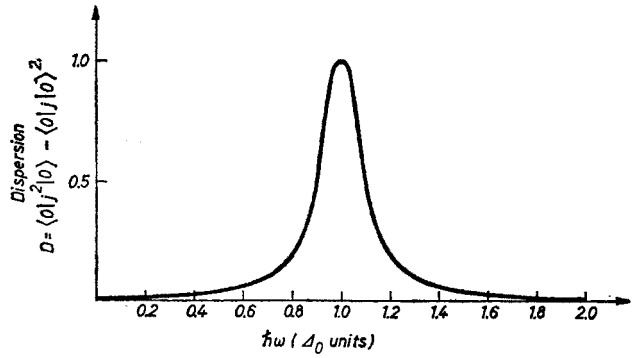

Fig. 3. Dispersion corresponding to the expected value of j_x operator calculated for the vacuum configuration in the "$j = 3/2$ shell" model

We can conclude that, in the approximation $\Omega \gg 1$, our system is entirely described by a single crossing of levels. The change in angular momentum is entirely due to the rearrangement of the HFB vacuum and the system does not respond to the rotation before and after crossing point. Let us emphasize, on the other hand, that for ω close to the crossing point usual HFB solutions become unphysical since the spread in angular momentum becomes large, contradicting the original assumption for the validity of the cranking model.

We have discussed regular (and continuous) solution of our model within approximation appropriate for $\Omega \gg 1$. However it is easy to find another solution of Eq. (3.6) which is exact in the case of $e = 0$. In this case we obtain

$$\frac{2\Delta}{G} = \frac{\Delta+\hbar\omega}{|\Delta+\hbar\omega|} + \frac{\Delta-\hbar\omega}{|\Delta-\hbar\omega|} + \frac{2\Delta\Omega}{\sqrt{\Delta^2+\varepsilon^2}}. \tag{3.23}$$

In the region of large ω we have simply

$$\Delta_{\text{right}} = \Delta_0 = \sqrt{(G\Omega)^2-\varepsilon^2} \tag{3.24}$$

and

$$\mathscr{E}_{\text{right}} = \mathscr{E}_0 = G\Omega. \tag{3.25}$$

This solution is valid for $\omega > \Delta_0/\hbar$. On the other hand, for small ω values we have

$$\Delta_{\text{left}} = \Delta_n, \tag{3.26}$$

$$\mathscr{E}_{\text{left}} = \mathscr{E}_n = \sqrt{\Delta_n^2+\varepsilon^2}, \tag{3.27}$$

where Δ_n is the solution of the equation

$$\frac{\Delta_n}{G} = 1 + \frac{\Omega\Delta_n}{\sqrt{\Delta_n^2+\varepsilon^2}}. \tag{3.28}$$

This solution is valid for $\omega < \Delta_n/\hbar$. Now, one can easily show that

$$\Delta_n > \Delta_0, \tag{3.29}$$

$$\mathscr{E}_n > \mathscr{E}_0 = G\Omega. \tag{3.30}$$

Consequently, in the region $\Delta_0/\hbar < \omega < \Delta_n/\hbar$ both the solutions coexist. We can also calculate the total energy E (Eq. (2.8)) of the system. Using (3.17) and (2.8) we obtain

$$E_{\text{right}} = -\Omega^2 G - \varepsilon^2/G \tag{3.31}$$

for $\omega > \Delta_0/\hbar$ and

$$E_{\text{left}} = -\Omega^2\mathscr{E}_n - \varepsilon^2\Omega/\mathscr{E}_n - \Delta_n \tag{3.32}$$

for $\omega < \Delta_0/\hbar$. Again, it is easy to prove that

$$E_{\text{right}} > E_{\text{left}}. \tag{3.33}$$

The results of this simple calculation are illustrated in Fig. 4 where both Δ and E are plotted versus ω. The energy jump illustrated in this figure and the fact that $\Delta_0 < \Delta_n$ may be tempting to join the two branches of the bottom part of Fig. 4 and thus providing the ex-

planation of the back-bending effect. In fact, the same properties of solutions seem to show up in more realistic situations (see below). However, we have seen that solutions corresponding to the transition (rearrangement) region, if exist, seem to be quite unphysical

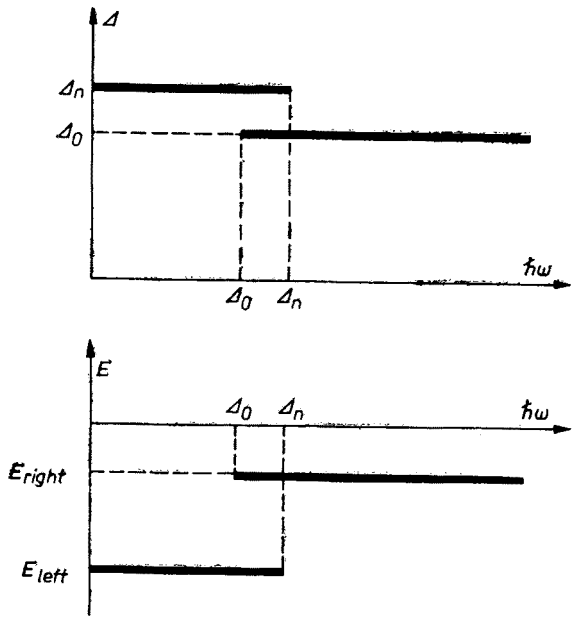

Fig. 4. Illustration of the non-unique character of the solutions of HFB equations applied to our simple model. Note that maximum two solutions coexist for a given ω value

as argued above (cf. Fig. 3). Consequently, we would rather look for the inclusion of the two quasiparticle states into the yrast line as the explanation of the physical effect of back-bending.

4. *Model based on the* $i\,^{13}_{2}$ *multiplet*

Let us examine another model which is believed to be slightly more realistic than the one discussed in the previous section. It is well known that in the realistic single particle nuclear spectrum one of the high angular momentum orbitals is usually shifted down to the lower nuclear major shell owing to the spin-orbit coupling. For example, in the deformed Rare Earth nuclei, the $i\,^{13}_{2}$ positive parity neutron orbital is embedded in the negative parity part of the spectrum. For instance, in the case of the harmonic oscillator spectrum, these negative parity states correspond to the major quantum number $N = 5$. Let us note that the embedded orbitals (e. g. $i\,^{13}_{2}$) are of relatively high angular momentum and thus are most sensitive to the nuclear Coriolis interaction. Consequently, we pay the special attention to the orbit $i\,^{13}_{2}$ assuming in our model, that the rest of the single particle states, say, $N = 5$ negative parity states, can be treated as a background

and can be approximated by a degenerate two-level model of the $j = \frac{3}{2}$ orbitals. Since the Coriolis matrix elements connect states of the same parity only, we may concentrate on $i\,{}^{13}_{2}$ orbitals separately. Consequently, we play with seven doubly degenerate levels, Fig. 5. We assume however, for the sake of simplicity, that the j_x matrix elements between these states are the same as in the case of spherical $i\,{}^{13}_{2}$ multiplet. Such an assumption

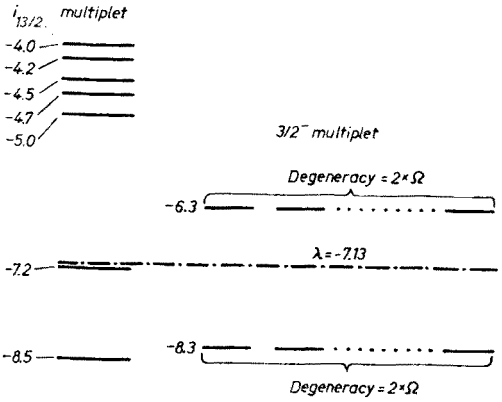

Fig. 5. Single particle level scheme used for illustration of the alignment effect within cranked HFB formalism. The positive parity multiplet i 13/2 is imitated by the set of seven levels (left-hand side) and the 2Ω times degenerate two-level sets serve as a model for $N = 5$ shell, the configuration characteristic for neutrons in Rare Earth nuclei. Numerical values correspond to the energies of the levels

introduces certain additional error which, for small deformations of realistic nuclei is of the order of a few percent and is expected to be of the order of errors introduced by the HFB approximation itself. The level positions are chosen somewhat arbitrarily so as to exhibit most drastically the effect of level crossing.

Before writing down the HFB equations for the model let us first introduce the Goodman transformation from the original basis of deformed orbitals $|k\rangle$, $|\bar{k}\rangle$ ... to the new basis, $|K\rangle$, $|\bar{K}\rangle$ ..., defined as follows

$$|K\rangle = \frac{1}{\sqrt{2}}[-|k\rangle + (-1)^{\Omega_k - \frac{1}{2}}|\bar{k}\rangle],$$

$$|\tilde{K}\rangle = \frac{1}{\sqrt{2}}[(-1)^{\Omega_k - \frac{1}{2}}|k\rangle + |\bar{k}\rangle], \tag{4.1}$$

with Ω_k being the projection of the single particle angular momentum on the nuclear symmetry axis [29]. Transformation (4.1) enables us to split the 28×28 matrix corresponding to the $i\,{}^{13}_{2}$ multiplet into two 14×14 sets of HFB equations

$$(e_k - \lambda)A_K{}^L - \hbar\omega \sum_{K'} (j_x)_{KK'} A_{K'}{}^L + \Delta B_{\tilde{K}}{}^L = E_L^{(\omega)} A_K{}^L,$$

$$-(e_k - \lambda)B_{\tilde{K}}{}^L - \hbar\omega \sum_{K'} (j_x)_{KK'} B_{\tilde{K}'}{}^L + \Delta A_K{}^L = E_L^{(\omega)} B_{\tilde{K}}{}^L \tag{4.2}$$

and

$$(e_k-\lambda)A_{\tilde{K}}^{\tilde{L}}+\hbar\omega\sum_{K'}(j_x)_{KK'}A_{\tilde{K}'}^{\tilde{L}}-\Delta B_K^{\tilde{L}} = E_{\tilde{L}}^{(\omega)}A_{\tilde{K}}^{\tilde{L}},$$

$$-(e_k-\lambda)B_K^{\tilde{L}}+\hbar\omega\sum_{K'}(j_x)_{KK'}B_{K'}^{\tilde{L}}-\Delta A_{\tilde{K}}^{\tilde{L}} = E_{\tilde{L}}^{(\omega)}B_K^{\tilde{L}}, \tag{4.3}$$

where the indices K, K', $\tilde{K}$, $\tilde{K}'$ run from 1 to 7 (see also below).

It is sufficient to solve only one of the above two sets since the substitution of $\{B_K^{\tilde{L}}, A_{\tilde{K}}^{\tilde{L}}; -E_{\tilde{L}}^{(\omega)}\}$ in place of $\{A_K^{\ L}, B_{\tilde{K}}^{\ L}; E_L^{(\omega)}\}$ in (4.2) transforms (4.2) into (4.3). This part of the HFB equations which corresponds to $j = 3/2$ two level model has known solutions (see Ref. [25]). They are coupled to the set (4.2) and (4.3) only through the particle number, gap, and angular momentum equations

$$N = \sum_K \varrho_{KK} \tag{4.4}$$

$$\Delta = 2G\sum_K \chi_{K\tilde{K}} \tag{4.5}$$

and

$$\hat{I} = \sum_{KL}(j_x)_{KL}\varrho_{KL} \tag{4.6}$$

which are common for both subsystems.

Matrices ϱ_{KL} and χ_{KL} are built out of the Bogoliubov transformation coefficients $A_K^{\ L}$ and $B_K^{\ L}$ appearing in the HFB equations (4.2) and (4.3)

$$\varrho_{KK'} = \sum_{\tilde{L}} B_K^{\tilde{L}}B_{K'}^{\tilde{L}}, \tag{4.7}$$

$$\varrho_{\tilde{K}\tilde{K}'} = \sum_L B_{\tilde{K}}^{\ L}B_{\tilde{K}'}^{\ L}, \tag{4.8}$$

$$\varrho_{K\tilde{K}'} = \varrho_{\tilde{K}K'} = 0, \tag{4.9}$$

$$\chi_{K\tilde{K}'} = \sum_{\tilde{L}} A_{\tilde{K}'}^{\tilde{L}}B_K^{\tilde{L}}, \tag{4.10}$$

$$\chi_{\tilde{K}K'} = \sum_L A_{K'}^{\ L}B_{\tilde{K}}^{\ L}, \tag{4.11}$$

$$\chi_{KK'} = \chi_{\tilde{K}\tilde{K}'} = 0. \tag{4.12}$$

Equations (4.2) and (4.3) are to be solved by iterative procedure for each ω value separately. Certain guess for λ and Δ is made first and the eigenvectors $A_K^{\ L}$ and $B_K^{\ L}$ are found from (4.2) and (4.3). Then matrices ϱ and χ are computed from Eqs (4.7)–(4.12) and selfconsistency relations (4.4) and (4.5) are checked. If equations (4.4) and (4.5) are not fulfilled, corrections to λ and Δ are to be made and the whole procedure is repeated. At the end of iteration we determine λ and Δ corresponding to the selfconsistency condition within prescribed accuracy. Then Eq. (4.6) is used to calculate $\hat{I}$.

Let us now discuss properties of the solutions of HFB equations and nature of the resulting back-bending effect in the framework of the model. Let us choose, for the sake of illustration, a definite set of numerical parameters. The corresponding single particle levels are plotted in Fig. 5. The location of the chemical potential λ is indicated in this figure for the case of $\omega = 0$. It corresponds to $G = 0.25$. The single particle level

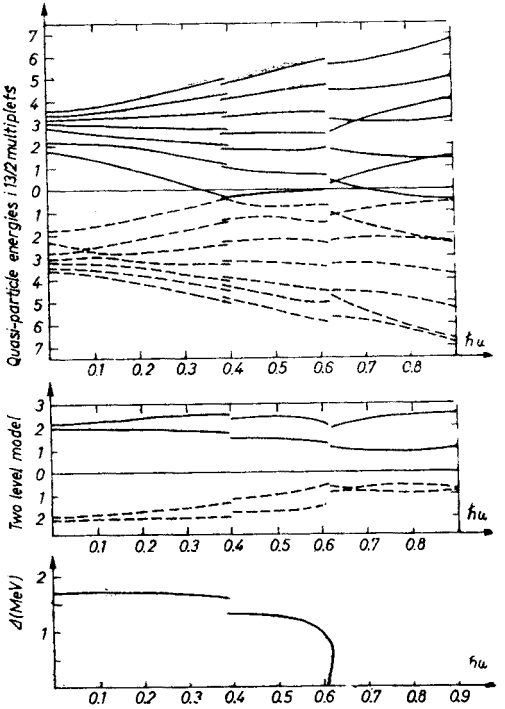

Fig. 6. The quasiparticle energies obtained with $G = 0.30$ MeV for the particle number $N = 12$. The single particle level spectrum is illustrated in Fig. 5. The corresponding behaviour of the energy gap Δ is shown in the bottom part of the figure. Note the two characteristic regions in the latter. They correspond to the jump in Δ (and in the quasiparticle spectrum), which reflects the gapless superconductivity effect, and to the region of disappearance of pairing ($\Delta \to 0$). The exact behaviour of the quasiparticle energies in the region $\Delta \to 0$ is described, in fact, by the multivalued functions and this cannot be illustrated in the scale of the figure

scheme is quite arbitrary and does not correspond to any realistic potential. The only condition we would like to fulfil is the approximate overlap of one of the levels with the location of the chemical potential λ. In such a case a gapless superconductivity (i. e. vanishing of the two quasiparticle energy) is especially distinct and easy to illustrate. Fig. 6 shows the quasiparticle eigenvalues $E_L^{(\omega)}$ obtained from the solution of set (4.2) of the HFB equations. Let us denote the eigenvalues by $E_7^{(\omega)}, E_6^{(\omega)}, \ldots, E_1^{(\omega)}, -E_{\tilde{1}}^{(\omega)}, -E_{\tilde{2}}^{(\omega)}, \ldots, -E_{\tilde{7}}^{(\omega)}$, in decreasing order. The eigenvalues of the second set (Eq. (4.3)) are therefore $E_{\tilde{7}}^{(\omega)}, E_{\tilde{6}}^{(\omega)}, \ldots, E_{\tilde{1}}^{(\omega)}, -E_1^{(\omega)}, -E_2^{(\omega)}, \ldots, -E_7^{(\omega)}$ (also in decreasing order). It is well known that the HFB formalism doubles artificially the number of dimensions of the

corresponding Hilbert space. Consequently, only part of the solutions can be interpreted as physical. It means e. g. that in the summations (4.7), (4.8), (4.10) and (4.11) indices L or $\tilde{L}$ run over the values corresponding to states included in this part. If, for instance, we chose the seven highest eigenvalues $E_L^{(\omega)}$ for each set (4.2) or (4.3) (i. e. solutions $E_7^{(\omega)}$, $E_6^{(\omega)}$, ..., $E_1^{(\omega)}$ for set (4.2) and $E_{\tilde{7}}^{(\omega)}$, $E_{\tilde{6}}^{(\omega)}$, ..., $E_{\tilde{1}}^{(\omega)}$ for set (4.3)) we obtain the vacuum which is stable with respect to the two quasiparticle excitations

$$E_{2\text{q.p.}}^{(\omega)} = E_{L_1}^{(\omega)} + E_{L_2}^{(\omega)}.$$

The stability of the vacuum means that $E_{2\text{q.p.}}^{(\omega)} > 0$; it is most easily seen in the region of small ω values where all the eigenvalues $E_7^{(\omega)}, E_6^{(\omega)}, \ldots, E_{\tilde{7}}^{(\omega)}$ are positive. The lowest two quasiparticle state is then

$$E_{2\text{q.p.}}^{(\omega)} = E_1^{(\omega)} + E_{\tilde{1}}^{(\omega)} > 0. \tag{4.13}$$

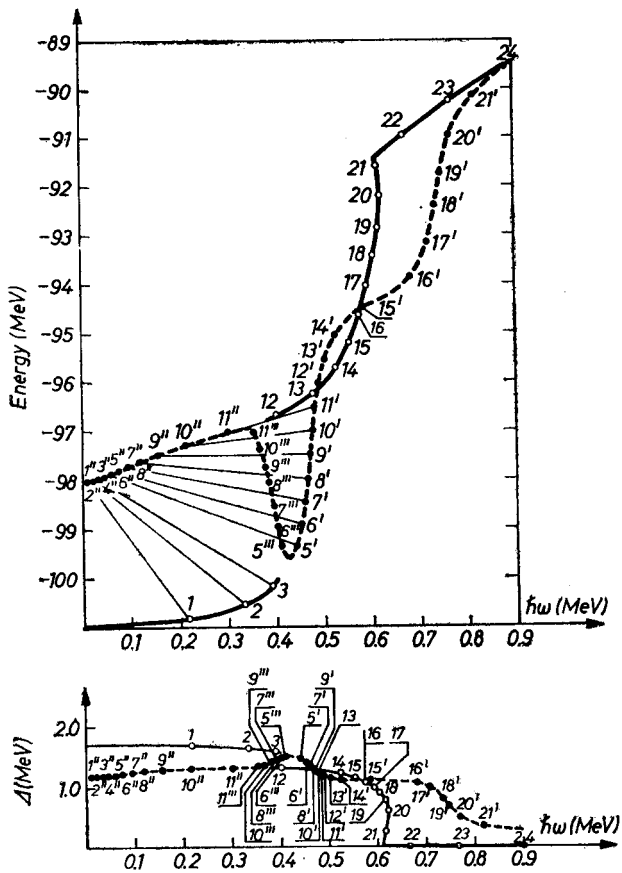

Fig. 7. Top part of the figure illustrates energy E versus angular velocity ω calculated within our model for the ground state configuration (original vacuum configuration, solid line) and for the two quasiparticle configuration (dashed line). Bottom part illustrates analogous variation of the parameter Δ. Numbers labeling the curves denote angular momentum (see text)

The same inequality holds even in the region of larger ω, where one of the eigenvalues becomes negative

$$E_I^{(\omega)} < 0.$$

This occurs in our example at $\omega \gtrsim 0.35$, Fig. 6, but as long as $E_I^{(\omega)} > -E_{\bar{I}}^{(\omega)}$, we still obtain inequality (4.13). The essential rearrangement in the vacuum appears at $\omega = \omega^* \approx 0.4$, Fig. 6, and this corresponds to a situation referred to as a gapless superconductivity. Beyond that point, characterised by vanishing of the lowest two quasiparticle excitation, the vacuum is not stable any more and the "new" vacuum, identified with the state of the lowest energy, is established: the extension of $E_I^{(\omega)}$ for $\omega > \omega^*$ has to be replaced by the extension of $-E_{\bar{I}}^{(\omega)}$ for $\omega > \omega^*$. In this way we are still in agreement with the rule that the highest eigenvalues have to be considered as physical and included in the vacuum state whose structure is thus rearranged at $\omega = \omega^*$. Since the two levels ($E_I^{(\omega)}$ and $-E_{\bar{I}}^{(\omega)}$ in Fig. 6) almost cross each other in our numerical example, the resulting transition in the vacuum is very rapid. Fig. 7 illustrates the energy E corresponding to this transition, calculated from Eq. (2.8). The resulting angular momenta, I, are also shown in the figure. We can see that there is a jump connected with the rearrangement in the vacuum, both in angular momentum and energy.

We have demonstrated in the previous section that the physical interpretation of the HFB solutions in an immediate vicinity of the transition point becomes rather uncertain (cf. Fig. 3); even if a solution of the cranked HFB equations exists in this region, it is composed of mixtures of states whose angular momenta differ very much from each other whereas the corresponding decomposition amplitudes are comparable and relatively large. For instance, in our example, the HFB wave function with the expectation value of spin $I = 6$ may contain large and comparable contributions from $I = 3$ and $I = 10$ components providing us with the proper average, $I = 6$. Consequently, the spread in angular momentum is large as it is shown in Fig. 3 for the simpler two-level model. In fact, in some part of the transition region it may even happen that there is no solution which would provide a continuous junction between the two branches marked in Fig. 7 with *1*, *2*, *3* and *12*, *13*, *14*, ..., respectively. Fig. 8 illustrates the fact that there is no junction between the two branches in the transition region when computed very thoroughly. We can see that the plot consists of the two disconnected parts similarily as in the simpler model discussed in preceding section (cf. Fig. 4).

Following the details of the computation one can see that behaviour of E and I vs ω near the transition region becomes extremely sensitive to the secondary features of the model and its parameters. Consequently, we have decided to remove this region out of our discussion considering it unphysical. We are left, in this way, with a considerable gap in the yrast line for angular momentum between *3* and *12* in agreement with the results of Hamamoto [18]. Now we can fill in the gap in the same way as we did it in Section 3 by considering the lowest two quasiparticle states. For this purpose we replace the eigenvalue $E_I^{(\omega)}$ by the closest one $-E_{\bar{I}}^{(\omega)}$ for $\omega < \omega^*$ obtaining in this way the two quasiparticle excitation which is shown in Fig. 7 as the branch marked with $I = 1''$, $3''$, $5''$, ..., $11''$.

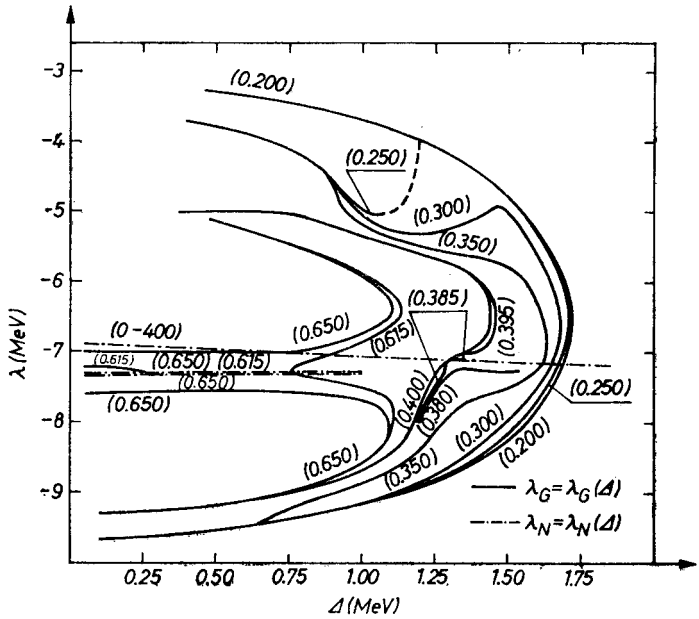

Fig. 8. Graphical illustration of the numerical solutions to the gap and particle number equations. Curves marked by $\lambda_N(\Delta)$ illustrate the dependence of λ on Δ found from the particle number equations, while these marked by $\lambda_G(\Delta)$ illustrate the analogous dependence following from the gap equations. The corresponding solutions of the HFB are represented in this plot by the crossing points of $\lambda_N(\Delta)$ and $\lambda_G(\Delta)$ curves. The values of $\hbar\omega$, in MeV, are indicated at each curve (numbers in parentheses)

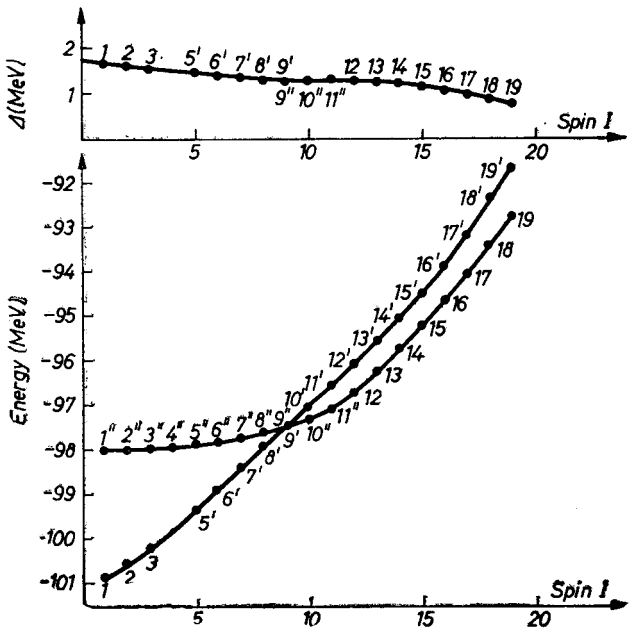

Fig. 9. Parameter Δ (top part) and energy E (bottom part) plotted as functions of angular momentum I

Similar extension into the region $\omega > \omega^*$ of the vacuum configuration valid for $\omega < \omega^*$ provides us with the branch *5'*, *6'*, ... (see Fig. 7). We can easily see that the new branches of the two quasiparticle nature form natural extensions of the two parts of the vacuum curve: branch *1*, *2*, *3* goes into *5'*, *6'*, ... while the branch *1''*, *2''*, ..., *11''* goes into *12*, *13*, ... The yrast states first belong to the lower line: *1*, *2*, *3*, *5'*, *6'*, ... until a certain state, *I'*, has the same energy as the one from the *I''* branch (for $I' = I''$); this fact obviously does not have to occur for integer angular momentum which in the whole formalism is treated as a nondiscrete variable. It can be seen that this occurs in our example roughly at $I = 9$ (i.e. the energies corresponding to points *9'* and *9''* are approximately equal) and this is just the position of the back-bending in our model. On the other hand, guided by the

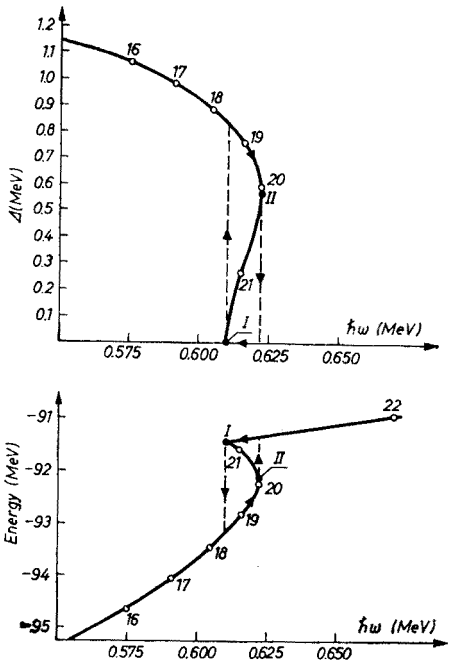

Fig. 10. The energy gap Δ (top part) and energy E (bottom part) versus angular velocity in the region of disappearance of pairing

discussion of the previous section, we again reject the whole transition region *11''*, *10'''*, ..., *5'''*, as unphysical. Thus we can see that the yrast line is not entirely built out of the HFB vacuum states in the region of back-bending; the two quasiparticle states form also a part of the yrast line in our approach. This is illustrated in Fig. 9 where the energy vs angular momentum is plotted. The existence of the crossing bands can easily be seen from this figure.

Let us finally discuss another possible region of the multivalued behaviour of the parameter Δ as a function of angular velocity ω and consequently the back-bending phenomenon that may show up according to our model. This region turns out to occur for

larger ω, say, above $\omega = 0.6$ in our numerical example, and is closely connected with the disappearance of the superfluid pairing correlations. One can show using simple arguments [28, 30] that a curve $\Delta = \Delta(\omega)$ may become multivalued near ω for which Δ tends to vanish (fast rotation limit). The same is obtained in our model provided that the pairing force strength G is large enough. The numerical results for the Δ versus ω curve are illustrated in Fig. 10 which contains also the energy E vs ω plot. Fig. 11 illustrates the same quantities as functions of angular momentum. Note that a single-valued behaviour results in this representation. One has to emphasize that the multi-valued behaviour of Δ versus

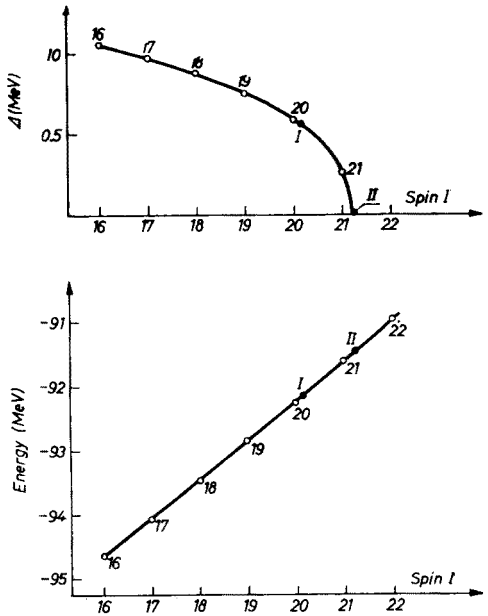

Fig. 11. Parameter Δ (top part) and energy E (bottom part) versus angular momentum I in the region of vanishing Δ

ω *in this part* of figure depends in a very sensitive way on the magnitude of the pairing force strength G as well as on the density of levels. It follows from our calculation that a value of G slightly smaller than that used in Figs 10 and 11 leads to a single-valued curve $\Delta(\omega)$ and, consequently, to no back-bending *in this* region. Thus, it is question of the detailed balance of various tendencies in real nuclei such as pairing force strength, density of levels, Coriolis strength etc. whether the vicinity of the transition point $\Delta \to 0$ provides us with the back-bending behaviour, or not.

5. *Conclusions*

We have calculated and discussed the dependence of energy E on angular velocity ω in the rotating nucleus. We have treated the rotation by means of the cranking model. We included the short range pairing interaction via Hartree-Fock-Bogoliubov formalism.

In order to obtain the illustrative results without getting involved into lengthy numerical computations we have employed two simple models which, we hope, are not too trivial so as they enable us to explain the nature of the rearrangement in HFB vacuum and the resulting back-bending effect.

Our main conclusion is that in the correct application of the cranked HFB method to nuclear rotation one has to take into account two quasiparticle states which are especially important in the region of the band crossing. It follows from considerations based on our models that the very sensitive (with respect to the details of the model and its parameters) solutions corresponding to the mixing between the two branches, (the vacuum and the two-quasiparticle excited ones) can be interpreted as unphysical and thus should be excluded out of the game. The back-bending effect itself turns out to result essentially as a rotational alignment of the quasiparticle states in line with the early prediction by Stephens and Simon [7]. However, the effect is closely connected with the decrease of the superfluid pairing correlations and the crossing of bands is closely connected with the effect of gapless superconductivity.

Our model predicts also a possibility of another mechanism of the back-bending effect viz. that arising in connection with the disappearance of pairing correlations. This, however, depends on the strength of the pairing force; the effect may take place only if the strength constant G of the pairing interaction is large enough.

REFERENCES

[1] C. C. Kistener, Eden Mateosian, A. W. Sunyar, to be published.
[2] I. Y. Lee, M. M. Aleonard, M. A. Delaplanque, Y. El-Masri, J. O. Newton, R. S. Simon, R. M. Diamond, F. S. Stephens, *Phys. Rev. Lett.* **38**, 1454 (1977).
[3] R. M. Lieder, H. Ryde, *Phenomena in Fast Rotating Nuclei*, to be published in *Adv. Nucl. Phys.*, Vol. **10**.
[4] R. Bengtsson, S. Frauendorf, Proc. Internat. Symposium on High Spin States and Nucl. Structure, Dresden, Sept. 1977, p. 74.
[5] R. Bengtsson, S. Frauendorf, Proc. Internat. Symposium on High Spin States and Nucl. Structure, Dresden, Sept. 1977, p. 76.
[6] A. Bohr, B. R. Mottelson, invited talk at the Internat. Conf. on Nuclear Structure, Tokyo 1977.
[7] F. S. Stephens, R. Simon, *Nucl. Phys.* **A183**, 256 (1972); F. S. Stephens, *Rev. Mod. Phys.* **47**, 43 (1975).
[8] A. Bohr, B. R. Mottelson, D. Pines, *Phys. Rev.* **110**, 936 (1958).
[9] B. R. Mottelson, J. G. Valatin, *Phys. Rev. Lett.* **5**, 511 (1960).
[10] D. R. Inglis, *Phys. Rev.* **96**, 1059 (1954); **97**, 701 (1955).
[11] A. Bohr, B. R. Mottelson, *Mat. Fys. Medd. Dan. Vid. Selsk.* **30**, no. 1 (1955).
[12] B. Banerjee, H. J. Mang, P. Ring, *Nucl. Phys.* **A215**, 366 (1973).
[13] P. C. Bhargava, D. J. Thouless, *Nucl. Phys.* **A215**, 515 (1973).
[14] P. C. Bhargava, *Nucl. Phys.* **A207**, 258 (1973).
[15] A. Faessler, K. R. Sandhya-Devi, F. Grümmer, K. W. Schmid, R. R. Hilton, *Nucl. Phys.* **A256**, 106 (1976).
[16] A. Goodman, *Nucl. Phys.* **A256**, 113 (1976).
[17] A. Bohr, suggestion made at the 4×50 Conference, June 1976, Copenhagen (unpublished).
[18] I. Hamamoto, *Nucl. Phys.* **A271**, 15 (1976).
[19] R. A. Sorensen, *Nucl. Phys.* **A269**, 301 (1976).

[20] E. R. Marshalek, A. Goodman, preprint 1977, to be published.
[21] A. Bohr, B. R. Mottelson, Nobel Lectures (1975); *Fys. Tidsskr.* **74**, no. 2 and 3 (1976).
[22] A. Goswami, L. Lin, G. L. Struble, *Phys. Lett.* **25B**, 451 (1967).
[23] R. Bengtsson, I. Hamamoto, B. R. Mottelson, NORDITA preprint, November 1977.
[24] S. Bose, J. Krumlinde, E. R. Marshalek, *Phys. Lett.* **53B**, 136 (1974).
[25] S. Y. Chu, E. R. Marshalek, P. Ring, J. Krumlinde, J. O. Rasmussen, *Phys. Rev.* **C12**, 1017 (1975).
[26] M. Baranger, *Phys. Rev.* **122**, 992 (1961).
[27] C. G. Andersson, S. E. Larsson, G. Leander, P. Möller, S. G. Nilsson, I. Ragnarsson, S. Åberg, R. Bengtsson, J. Dudek, B. Nerlo-Pomorska, K. Pomorski, Z. Szymański, *Nucl. Phys.* **A268**, 205 (1976).
[28] Z. Szymański, lectures delivered at École d'Été de Physique Théorique, Les Houches 1977, to be published.
[29] A. Goodman, *Nucl. Phys.* **A230**, 466 (1974).
[30] R. A. Sorensen, Proc. Orsay Colloquium on Intermediate Nuclei, July 1971.